HHS Public Access

Author manuscript

Int J Comput Assist Radiol Surg. Author manuscript; available in PMC 2015 December 10.

Published in final edited form as:

Int J Comput Assist Radiol Surg. 2015 May ; 10(5): 637–650. doi:10.1007/s11548-014-1102-0.

Preclinical Feasibility of a Technology Framework for MRI-guided Iliac Angioplasty

Martin A. Rube, MSc[1], **Fabiola Fernandez-Gutierrez, MSc**[1], **Benjamin F. Cox, MD**[1], **Andrew B. Holbrook, PhD**[2], **J. Graeme Houston, MD, FRCP, FRCR, EBIR**[3], **Richard D. White, MBChB, FRCR**[3,4], **Helen McLeod, BSN**[1,3], **Mahsa Fatahi, MSc**[1], and **Andreas Melzer, MD, DDS**[1]

[1] Institute for Medical Science and Technology, Division of Imaging and Technology, University of Dundee, Dundee, United Kingdom Wilson House, 1 Wurzburg Loan, DD2 1FD Dundee, United Kingdom

[2] Department of Radiology, Stanford University, Stanford, CA, United States 1201 Welch Rd, Stanford, CA 94305, United States

[3] Department of Clinical Radiology, Ninewells Hospital and Medical School, NHS Tayside, Dundee, United Kingdom Ninewells Hospital & Medical School, DD1 9SY Dundee, United Kingdom

[4] Department of Clinical Radiology, University Hospital of Wales, Cardiff, United Kingdom Heath Park, CF144XW Cardiff, United Kingdom

Abstract

Purpose—Interventional MRI has significant potential for image guidance of iliac angioplasty and related vascular procedures. A technology framework with in-room image display, control, communication and MRI-guided intervention techniques was designed and tested for its potential to provide safe, fast and efficient MRI-guided angioplasty of the iliac arteries.

Methods—A 1.5T MRI scanner was adapted for interactive imaging during endovascular procedures using new or modified interventional devices such as guidewires and catheters. A perfused vascular phantom was used for testing. Pre-, intra- and post-procedural visualization and measurement of vascular morphology and flow was implemented. A detailed analysis of X-Ray fluoroscopic angiography workflow was conducted and applied. Two interventional radiologists and one physician in training performed 39 procedures. All procedures were timed and analyzed.

Results—MRI-guided iliac angioplasty procedures were successfully performed with progressive adaptation of techniques and workflow. The workflow, setup and protocol enabled a reduction in table time for a dedicated MRI-guided procedure to 6 min 33 s with a mean procedure time of 9 min 2 s, comparable to the mean procedure time of 8 min 42 s for the standard X-Ray guided procedure.

Corresponding author: Martin Rube, Institute for Medical Science and Technology, University of Dundee, Wilson House, 1 Wurzburg Loan, DD2 1FD, Dundee, United Kingdom, Fax: +44 (0) 1382 386588; Phone: +44 (0) 1382 388355; martin.a.rube@gmail.com.

Conclusions—MRI-guided iliac vascular interventions were found to be feasible and practical using this framework and optimized workflow. In particular the real-time flow analysis was found to be helpful for pre- and post-interventional assessments. Design optimization of the catheters and in vivo experiments are required before clinical evaluation.

Keywords

interventional MRI workflow; device localization; catheter tracking; MR-guided balloon angioplasty

INTRODUCTION

X-Ray fluoroscopy-guided catheter-based procedures are state of the art treatment of cardiovascular disease. X-Ray provides high temporal and spatial resolution, is cost-effective and widely available. Limitations of X-Ray are poor visualization of soft tissues (such as those of the cardiovascular system) and the need for nephrotoxic and allergenic iodine-based contrast media [1]. Interventions can be time-consuming resulting in significant ionizing radiation dosage, which can accumulate for the patient throughout the procedure(s) [2]. Moreover, clinical staff working in an angiography suite can be exposed to radiation [2] from several procedures every day.

Magnetic Resonance Imaging (MRI) provides high soft tissue contrast, soft tissue characterization, fast and true multi-planar imaging in arbitrary orientations, temperature monitoring, functional information and near real-time imaging (rtMRI) capability without exposure to ionizing radiation. Interventional MRI (iMRI) would provide instant evaluation of many therapeutic goals throughout the intervention [3]. However, the interventional workflow is greatly compromised by complex MRI operation, limited communication with and access to the patient, high acoustic noise levels and the requirement to ensure MRI safety throughout a procedure [4]. At present, dedicated training facilities and programs are not available. As a consequence of these problems, MRI has not been widely accepted for guiding interventions.

With current technological advances (such as novel scanner designs, which are shorter and more open [5]), new interactive rtMRI interfaces [6–9] and new MRI-safe key devices such as guidewires [10] have addressed many of those challenges. Accordingly, iMRI has the potential to be accepted in routine clinical practice. However, there are still several challenges and problems to be solved:

(i) Real-time guidance

Instant image display, similar to fluoroscopy or ultrasound-guided procedures, is a necessity for any image-guided procedure and is also a key requirement for iMRI. Closed-loop control of image acquisition and in-room display opens a new dimension [11] for interactive imaging. Generally, scanner manufacturers provide product (i/Drive Pro Plus [6], GE Healthcare, Waukesha, WI, USA) or work in progress (Interactive Front End [8] (Siemens, Erlangen, Germany) and eXTernal Control [7] (Philips Healthcare, Best, the Netherlands)) rtMRI implementations with continuous data acquisition and image display. These

applications, however, allow very limited selection of pulse sequences and only basic modifications of parameters during imaging. Unlike product systems, we would like to demonstrate the additional value and utility of a more flexible research platform (RTHawk, HeartVista, Palo Alto, CA, USA) that allows for fundamental changes of the image acquisition scheme during MRI scanning [9].

(ii) Device visualization and tracking

Most commercially available cardiovascular interventional devices, such as catheters, guidewires or implants, are not designed with MRI compatibility [4, 12] in mind. Accordingly, all iMRI devices for this study were developed or modified in-house. MRI-safe and compatible (non-metallic) materials are usually difficult to identify on MR images [13], therefore suitable visualization techniques are required to locate and guide the instrument to the intended target area. We propose using passive markers [14] for polymer-based guidewires and resonant markers [15] for catheter visualization during cardiovascular iMRI.

(iii) Interactive MRI remote control

An integral part of the iMRI workflow is that the physician (in the scanner room) manipulates interventional devices and the scanner operator (in the control room) adjusts the scan acquisition parameters to identify the device and its manipulations. However, adjustments can require multiple gestures, intense discussion between operator and physician (if a communication system is in place) or may necessitate the operator stopping/pausing the scan to enter the scanner room. This can cause significant workflow interruptions and delays. Major changes to the scan acquisition (e.g. change of pulse sequence) can cause additional delays because the current scan must be aborted and a new scan restarted, including adjustment of parameters, pulse sequence download and pre-scanning processes. To overcome these workflow interruptions and to provide intuitive and flexible control at the patient bed, we implemented a wireless in- room operator control system based on mobile tablet devices in combination with the aforementioned rtMRI interface.

(iv) Communication

Previous studies [16, 17] have demonstrated that gradient noise of current MRI scanners obstructs communication between physician, assisting staff and scanner operator. Preceding experiments have identified that this creates a major workflow challenge, resulting in a significant increase in intervention time and safety concerns. We have implemented a concept for wireless communication and MRI scanner remote.

(v) Workflow optimization and training

In contrast to most previous attempts to perform MRI-guided cardiovascular interventions, we propose to start by initially applying our iMRI framework to uncomplicated common iliac balloon angioplasty procedures and not to challenging cardiovascular interventions (such as electrophysiology mapping during catheterization [18, 19]). Our research approach involved detailed analysis and comparison of the equivalent workflow from the X-Ray

angiography suite regarding staffing, time, utilized devices, patient safety, and clinical efficacy.

The objective of this study was to develop an improved framework of technologies to address the aforementioned obstacles for iMRI and to validate safe, fast and efficient solely MRI-guided angioplasty of the iliac arteries in a perfused vascular phantom.

MATERIALS AND METHODS

All experiments were conducted in a multi-modality setup (see Fig. 1) consisting of a digital subtraction angiographic (DSA) unit (OEC 9900 Elite, software release 7.0.31, GE Healthcare, Waukesha, WI, USA) and a 1.5 T MRI unit (Signa HDx, software release 15.0M4A, GE Healthcare, Waukesha, WI, USA). The units are located in two adjoining rooms, interconnected with shielded sliding doors that allow patient transfer between the units on a mobile table with radiolucent sliding table top (MR 1050 surgical suite, GE Healthcare and Maquet, Rastatt, Germany). During MRI-guided procedures, the X-Ray system in our facility is still available for preparation, backup or emergencies.

MRI scanner remote control and communication

Two-way data communication between the MRI scanner and an external Linux (Ubuntu 11.10 64bit) workstation (z820, Hewlett-Packard, Palo Alto, CA) was accomplished via Gigabit Ethernet (Fig. 1). An rtMRI software framework (RTHawk, Version 0.9.28, HeartVista, Inc., Los Altos, CA, USA) was employed for rtMRI reconstruction, display and interactive scan control. A shielded 40″ LCD monitor (Multeos 401, NEC Corporation, Tokyo, Japan) was adopted for in-room display of MR images, which were transferred via fibre optic cables (M1-1000, Opticis, Sungnam City, Korea).

The multi-modality suite was also equipped with a wireless network connection for data transfer and communication (Fig. 1). The wireless network connection was established with a modified router (DIR615, D-Link, Taipei, Taiwan), with one antenna positioned in the magnet room and the other one outside the Faraday cage, providing a stable network connection throughout both areas.

To provide the vast majority of control in the procedure room, we implemented a wireless in- room operator control system based on a mobile tablet device (iPad 1, Apple, Cupertino, CA, USA). This tablet computer, mounted on a modified MRI-safe intravenous (IV) fluid-holder pole, enabled the physician to interact directly with the MRI scanner and/or the real-time system on the external workstation, to trigger data acquisition and also adjust the acquisition scheme (scan parameters, scan plane geometry and pulse sequence). Communication between tablet PC and Linux workstation was established via Virtual Network Computing (VNC). This setup (see Fig. 2 a and b) allowed the physician and operator to make real-time changes to the scan sequence parameters to follow the manipulation of devices on the fly. Moreover, we utilized a second tablet device (iPad 3, Apple, Cupertino, CA, USA) for wireless audiovisual communication via Voice over Internet Protocol (Skype, Luxembourg City, Luxemburg). In combination with a Bluetooth headset (Calisto B70, Plantronics, Santa Cruz, CA, USA), positioned under the noise

protection earmuffs, the scanner operator and the physician were able to communicate. Each tablet device was inserted into a plastic cover to simulate sterile conditions, while the physician was still able to operate the touch screen with latex gloves.

Interventional Devices

The interventional devices for this study (see Fig. 3 a - c) were selected according to MRI compatibility and were modified or developed in-house. Passive markers based on superparamagnetic iron-oxide (SPIO) nanoparticles were employed for guidewire visualization and resonant markers were used for catheter visualization. All devices were previously found compliant [10, 20, 21] with the relevant ASTM standards [4] (F2182-09, F2052-06, F2213–06, F2119-07) with regards to RF-induced heating, MRI safety and imaging artefacts.

Guidewires—For X-Ray-guided interventions, commercially available 0.035″ guidewires (Standard Glidewire, Terumo, Somerset, NJ, USA) were used. For MRI-guided interventions, a novel hydrophilic-coated and MRI-safe guidewire prototype that was developed with EPflex GmbH (Dettingen / Erms, Germany) was used, with a diameter of 0.035” and a length of 120 cm. The Polyether ether ketone (PEEK)-based guidewires were prepared [10] and tested [20] for MRI as previously described. SPIO nanoparticles in a coating (MagnaFy, Nano4imaging GmbH (Aachen, Germany)) were incorporated into the Polyether Block Amide (PEBAX) tip material (see Fig. 3a) at distinct locations (one marker (~1 mm length) at the tip and then five markers (~1 mm length) at 2 cm intervals). These passive SPIO markers allow for passive visualization of the guidewire tip based on a local change in susceptibility and the resulting signal void at each marker location [14].

Catheters—Commercially available non-braided catheters have been tested and those found safe and compatible in the MRI environment (see list below) were selected and prepared for iMRI visualization (see Fig. 3b). We equipped each catheter with a resonant circuit, composed of a rectangular planar spiral coil (wound with enamelled copper wire) and a non-magnetic ceramic SMD-capacitor (43 - 56 pF, 1.0 mm × 0.5 mm × 0.6 mm, Vishay Intertechnology, Inc., Malvern, PA, USA). The resonant circuit was then tuned to 63.8 MHz (the Proton Larmor frequency at 1.5 T) in 0.9% saline solution using a spectrum analyser (HM5014-2, HAMEG, Mainhausen / Rhein, Germany). The resonators were crimped to the distal part (5 mm from the tip) of the catheter and coated with medical grade heat shrink tubing (Advanced Polymers, Salem, NH, USA). We measured a quality factor of 35 - 50 with the resonant circuits attached to the catheters. In their entirety, a resonant circuit (including coil, capacitor and coating) had an average length of 10 mm. The resonant circuit also led to an increased outer catheter diameter of maximum 7-French (2.67 mm)

- 5-F Straight catheter (Beacon Tip Royal Flush, Cook Inc., Bloomington, IN, USA), length 70 cm (lumen 0.035”)
- 6-F Multipurpose catheter (Soft-Vu, AngioDynamics, Latham, NY, USA), length 90 cm (lumen 0.035”)
- 5-F PTA Balloon catheter (Workhorse II, AngioDynamics, Latham, NY, USA), length 75 cm (lumen 0.035”), balloon 10 mm × 4 cm

Phantoms

In vitro experiments were conducted on an arterial vessel phantom consisting of linked femoral, abdominal and thoracic modules (L-F-S-Left-003, A-S-N-001, T-R-N-020, Elastrat, Sarl, Switzerland). A neonatal blood pressure cuff (SoftCheck Neonatals, Statcorp Medical, Jacksonville, FL, USA) was secured to the right common iliac artery (with electrical tape and rubber sheet). The pressure cuff (arrowhead in Fig. 4) was inflated with water to occlude the artery. The resistance was optimized in order to allow passive deflation with angioplasty balloon expansion.

The phantoms were placed in the supine position on the MRI-safe sliding table top. A heart-lung machine (HL-30, Maquet, Rastatt, Germany) was then connected to the arterial model. One HL-30 D150 pump was customized to work with a single roller head in order to mimic (pulsatile) physiologic flow. The model was connected to the pump as demonstrated in Fig. 4. Inflow was connected to the model's cardiac chamber (arrow in Fig. 4c) and outflow was achieved with dual upper (neck and arm) and lower (everywhere else) systems (Fig. 4a and b). System pressure was controlled using a non-operational D150 pump occlusion knob on the lower system outflow tube in order to mimic systolic / diastolic pressures. The master arterial flow pump was set to a flow rate of approximately 5.5 litres per minute, a heart rate of 85 - 95 beats per minute and a blood pressure of approximately 130 / 70 mmHg. Vascular access was established with a 12-F introducer sheath (Check-Flo, Cook Inc., Bloomington, IN, USA) (indicated by a '+' in Fig. 4), inserted into the right femoral artery. All vessels, tubing and the pump reservoir were filled with 0.9% saline solution to mimic the electrical properties of blood. Furthermore, each container of the vessel phantom modules was backfilled with a 10% gelatinous solution to improve the MRI vascular visualization. The heart-lung machine was positioned in the X-Ray angiography suite (see Fig. 1) to prevent interference with the MRI system. For MRI experiments, however, the phantom was connected to the vessel model via tubing (see Fig. 1 and 4), passing the Faraday cage through the wave-guides. Silicon tubing (PT 12.7×3.2, Silex, Bordon, UK), with an inner diameter of 16 mm and length of 5 m, was utilized for the inflow as well as the outflow, for both the X-Ray and MRI experiments.

Study Protocol

Percutaneous balloon angioplasty is a technique widely used to treat iliac artery stenosis or occlusion. A detailed analysis of the equivalent workflow from the X-Ray angiography suite was conducted according to a protocol that was previously described elsewhere [22]. In this study, two trained interventional radiologists (one consultant and one final year trainee (SpR / Registrar)) and one physician in training performed 39 procedures in 6 sessions. Nine X-Ray-guided procedures and 30 MRI-guided procedures were performed. All procedures were performed according to the protocol described in Fig. 5 and the time for each step was recorded. Analysis of variance (ANOVA) was used ($p=0.05$) to test the effects of the protocols, the clinicians and the interaction effect between protocols and clinicians on the procedure time.

The clinical protocol employed for X-Ray-guided common iliac angioplasty is displayed in Fig. 5a. With increasing experience the DSA protocol was adapted to the MRI environment and the steps were adjusted to the final MRI protocol, which is demonstrated in Fig. 5b.

At the beginning of each session, a set of X-Ray-guided procedures was performed as a reference for the subsequent experiments. Each person in the room was wearing lead aprons for radiation protection. The phantom was then transferred into the MRI room. During the MRI-guided intervention, a trained MRI technologist or researcher operated the scanner. In addition the physician, who had visual and audio contact with the operator, was able to make the required adjustments with the mobile tablet device.

X-Ray Imaging—X-Ray-guided common iliac angioplasty procedures were performed using the OEC 9900 C-Arm (GE Healthcare, Waukesha, WI, USA) according to the protocol of the two interventional radiologists (see Fig. 5a). X-Ray contrast agent (Omnipaque 300; Schering, Vienna, Austria) diluted in 0.9% saline solution (50:50) was injected into the balloon catheter for visualization and to verify correct placement. After the balloon catheter was removed, a straight catheter was inserted and DSA was performed with a bolus of contrast agent to evaluate the results.

MR Imaging—All MR images were obtained using a dedicated interventional coil prototype “DuoFlex Coil Suite” which was developed in collaboration with GE Healthcare (Waukesha, WI, USA) and MR Instruments Inc. (Minneapolis, MN, USA). The coil consists of two interchangeable parts, which can be plugged into a connector box. For this study, we used a four-channel phased array element, which was positioned posteriorly and a one-channel single loop element, which was positioned anteriorly. The imaging parameters are summarized in tables 1 and 2 and were acquired without breath hold or cardiac triggering. After the pre-interventional diagnostic scan sequences, we used an interactive rtMRI sequence during device manipulation. During the intervention, diagnostic images were only acquired on request of the physician. At first we performed the interventions using the product rtMRI protocol (see MR Imaging – Product Protocol) and later on with the developed rtMRI protocol (see MR Imaging – Research Protocol), both with communication between operator and physician.

MR Imaging –Product Protocol: Diagnostic imaging, based on high-resolution fast spoiled gradient echo (FSPGR) and Time of Flight (ToF) MR angiography (MRA), was performed for pre-interventional assessment and procedure planning. During the intervention, interactive fast gradient echo (FGRE) or FSPGR images were acquired using the product rtMRI interface (i/Drive Pro Plus, GE Healthcare, Waukesha, WI, USA). For visualization of the expanded endovascular balloon, a 0.9% saline solution doped (1:100) with a Gadolinium (Gd)-based MRI contrast agent (Magnevist, Beyer-Schering Pharma AG, Berlin, Germany) was injected into the catheter. This enabled us to depict the balloon in a T_1-weighted FSPGR sequence. After the procedure, we performed a high-resolution FSPGR and a ToF MRA to verify the technical success while keeping the guidewire in place. All pulse sequences and imaging parameters are displayed in table 1.

MR Imaging – Research Protocol: For our study we employed the research software framework RTHawk (Version 0.9.28, HeartVista, Inc., Los Altos, CA, USA), which allows the generation of new pulse sequences and dynamically change major aspects of data acquisition such as gradient waveforms, excitations and scan geometry on the fly [9]. We performed diagnostic imaging, based on high-resolution FSPGR and a real-time flow analysis (rtFLOW) with bipolar velocity-encoding gradients and a spiral k-space acquisition scheme for pre-interventional assessment, procedure planning and stenosis assessment. In consensus with the interventional radiologists, we increased the spatial resolution for the sequences with a Cartesian readout scheme and reduced the k-space coverage in the phase encoding direction (ky = 62%) and employed zero filling [23] to decrease scan time. During the intervention we were able to switch on the fly between various pulse sequences including the rtFLOW sequence. We used a balanced steady state free precession (bSSFP) sequence, in which blood appears bright (enabling identification of blood vessels without the need for a contrast agent), or alternatively an FGRE for guidewire manipulation. The developed rtMRI user interface allowed interchange between: a (T_2/T_1 weighted) Cartesian bSSFP for high spatial resolution and a spiral bSSFP for high temporal resolution; an FGRE sequence, which is particularly useful for visualization of the resonant markers on the catheter; and a (T_1-weighted) FSPGR for visualization of the inflated balloon. The 0.9% saline/Gd-based contrast agent solution for injection into the balloon catheter was the same as used in the product protocol. The flip angle was varied (15 - 60°) depending on which device would be advanced and the anatomical location examined. It was set to 30° or lower for catheter visualization and to 60° for T_1 weighting for visualization of the inflated balloon catheter. At the end of each procedure the outcome was assessed, with a similar protocol as during the planning stage, with flow analysis in the target section and high-resolution diagnostic imaging. All employed pulse sequences and imaging parameters are reported in table 2.

RESULTS

In the present study, guidewire positioning was feasible, as was selective catheterization of the common iliac artery, with the proposed visualization techniques. Over-the-wire positioning of the catheters was possible, as were consecutive balloon angioplasties after removal of the guidewire (n = 39 out of 39). The average procedure times and the range per radiologist are shown in Fig. 6.

X-Ray - Guided Intervention

The mean procedure time for all X-Ray guided interventions (n = 9) was 8 minutes and 42 seconds (ranging from 6 minutes and 32 seconds to 10 minutes and 51 seconds). The accumulated average X-Ray radiation dose for all three procedures per radiologist was: 0.131 $mGym^2$ (trained interventional radiologist – consultant level); 0.147 $mGym^2$ (trained interventional radiologist – SpR/Registrar); and 0.139 $mGym^2$ (physician in training).

MRI - Guided Intervention

During guidewire positioning in the aorta, the rtMRI FGRE sequence was used with a flip angle of 30° for good visualization of the passive markers. During catheter insertion, the

resonant coil led to strong visual local signal increase during interactive real-time FGRE imaging with a flip angle of 15°. This allowed for fast placement of the catheter in the targeted vessel segment. Signal enhancements during imaging with low flip angles were more pronounced than with equivalent sequences with higher flip angles.

Fig. 7 shows the device visualization during various steps of the balloon angioplasty with the standard GE console (Fig. 7a) and the product rtMRI interface (i/Drive Pro Plus, GE Healthcare, Waukesha, WI, USA) (Fig. 7b - d) and Fig. 8 shows the MR images during the advanced research protocol. Fig. 7a shows a maximum intensity projection (MIP) of a 2D ToF MRA obtained in axial slice orientation without any device present. Fig. 7b displays the tip section of the MRI-safe guidewire (the arrow illustrates the guidewire tip) positioned in the abdominal aorta. The resonant marker (arrowhead) on the straight catheter can be identified in Fig. 7c as a white spot high up in the right common iliac artery. Fig. 7d displays the inflated balloon (indicated by a '+') catheter (1:100 Gd-doped saline solution) that had been placed just above the common iliac artery and required re-positioning.

Fig. 8a shows the guidewire, visualized with the passive markers (the arrow illustrates the passive marker on the guidewire tip), which had been advanced through the iliac arteries and positioned in the abdominal aorta during imaging with the advanced research protocol. The image also shows a turbulent flow pattern secondary to the connector distal to the renal arteries. Fig. 8b shows the resonant marker (arrowhead) on the straight catheter, advanced over the guidewire and positioned at the level of the simulated stenosis in the common iliac artery. Fig. 8c shows a high flip angle image with the expanded Gd-filled balloon (+) catheter at the stenosed section of the common iliac artery. The signal enhancement of the resonant marker on the balloon catheter allowed for simple and fast positioning of the balloon catheter in the target area. Inflating the balloon with a Gd-doped saline solution and changing the flip angle to 60° to achieve T_1-weighting enabled good intra-arterial balloon position verification. Fig. 8d shows a MIP of a 2D ToF MRA after the stenosis has been treated. A drastic decrease in velocity (peak velocities of 20 – 25 cm/s pre-treatment and 10 – 12 cm/s post-treatment) was observed with the rtFLOW assessment post treatment (Fig. 9b) of the stenosis, as compared to Fig. 9a, which was obtained pre treatment.

The catheters and guidewires along with their applied markers showed no macroscopic evidence of fracture or kinking and the catheters remained patent. The operators and physicians agreed that the catheter and guidewire position in the MR images was identified easily and reliably on all occasions (n = 30 out of 30).

The averaged procedure time per radiologist and the range (illustrated as bars) are presented in Fig. 6. The mean procedure time for all MRI-guided interventions with the product protocol (n = 5 per radiologist) was 19 minutes and 58 seconds (range 13 minutes and 32 seconds to 28 minutes and 34 seconds). The mean procedure time with the research protocol (n = 5 per radiologist) was 9 minutes 2 seconds (range 6 minutes and 33 seconds to 11 minutes and 23 seconds) with the research protocol (n = 5 per radiologist). The physicians rated the ergonomics for endovascular device placement (see Fig. 10b) during MRI scanning as being tolerable.

ANOVA showed significant difference between the protocols and also between the clinicians. Pairwise comparisons showed a significant difference between the MRI-Product Protocol and the other two protocols and no significant difference between the X-Ray and the MRI-Research Protocol. Pairwise comparisons showed a significant difference between the consultant interventional radiologist and the other two clinicians. No significant difference was found between SpR/Registrar and physician in training. ANOVA showed no significance when considering the interaction effect between protocol and clinician.

DISCUSSION

This work demonstrates the preclinical feasibility and efficiency of common endovascular interventions (such as balloon angioplasty of the common iliac artery) under MRI guidance. A combination of optimized workflow, suitable technologies for communication, in-room visualization and remote control of the MRI scanner, and safe and readily visualized endovascular devices, enabled satisfactory and effective interventions. This may be a first step towards standardization to facilitate training of MRI-guided techniques.

Interventional Devices

Endovascular interventions require iterative use of guidewires and catheters, as well as device exchanges with one or the other in place. Inductively coupling resonant circuits provide an RF-safe alternative positive contrast technique [15] and are easy to depict on MR images [24]. The main benefits are that resonant circuits are technically simpler compared to active tracking coils [13]. Low profile resonant circuits have the potential for integration into the commercial production of catheters [25] as no physical wire connection to the MRI scanner is required.

New interventional catheters can be developed specifically for use during MRI-guided procedures with multiple resonant markers along the catheter to provide visualization of longer catheter segments [26]. We have selected non-braided angiographic catheters, which are MRI-safe but have little torque and limited navigation characteristics. This was not an issue for common iliac artery angioplasty but could be problematic for more challenging endovascular interventions.

A limitation of the catheters that we used in this study is the resonant marker design, which was applied to the surface of the catheters and therefore increased the outer diameter and stiffness of the device. This would necessitate arterial access of a larger calibre than would normally be performed and potentially limits the use of these catheters to interventions in larger vessels only. However, the increased stiffness and outer diameter are temporary problems relating to manually produced resonant circuits. Recently, micro systems-based technologies for producing resonant circuits have been validated [25] and fully integrated designs have been proposed [25], which would allow for complete integration under the final coating of catheters.

The coil and capacitor dimensions, which are required to achieve a sufficient quality factor (greater than 15), limit the use of such resonant circuits for devices with a small outer diameter (below 1 mm). At present, this restricts the use of this technology to guidewires

with an outer diameter of 0.038” or less. An alternative approach for device visualization in iMRI is to use magnetic susceptibility markers [14] i.e. superparamagnetic nanoparticles [10]. Although susceptibility-based visualization of a guidewire marked with passive markers is more difficult to depict on MRI as it causes a signal void, it was found to be sufficient for navigation during all interventions performed in the current study. However, in small vessels or next to air-filled cavities (which also give signal voids), a more flexible contrast method would improve device localization.

During MRI-guided interventions, the MRI-safe guidewire was considered satisfactory, with a similar performance to commercially available guidewires for X-Ray fluoroscopy, as verified by the interventional radiologists. Further studies are needed to fully assess the mechanical performance of this new MRI-safe guidewire that received the CE mark in October 2012.

Both device visualization techniques employed in this study did not require a physical connection between the device and the MRI scanner, thereby simplifying instrument handling as well as avoiding unintended RF coupling effects, which constitute local heating risks for the patient [27, 28]. It has previously been shown that the guidewires [20] and the resonant markers on the catheters [21], which were used in this study, did not cause a significant temperature rise during worst case heating experiments.

Interventional MRI Setup

The limited patient access in closed-bore magnets provides a significant challenge for MRI-guided interventions, particularly if the physician has to reach into the isocenter of the MRI scanner e.g. for needle insertion [5, 29]. For endovascular interventions, however, the access site is mainly via the common femoral artery and only the treatment area is positioned in the centre of the bore. This allows the physician to be situated in front of the MRI scanner while inserting endovascular devices (Fig. 2 and 10b). In our study, all physicians agreed that this position was tolerable throughout the procedures and the scanner display and control within arm reach (Fig. 10c) was considered to be useful. Moreover, the ergonomic component and access to the patient could be improved by using a shorter and more open MRI scanner design. However, a detailed study is required to evaluate these modifications as well as long-term ergonomic effects.

Another hurdle to be overcome is the need to simplify receive coil positioning while a sterile iMRI environment is maintained. The interventional coil prototype facilitated fast and reliable coil positioning (see Fig. 10a) while enabling suitable quality interventional imaging for a relatively large field of view (FOV). Imaging and positioning of standard imaging coils, such as an eight-channel body array coil, was found to be time-consuming and could also prove challenging in terms of maintaining sterility around the puncture site. This problem has been addressed with a new interventional coil design (DuoFlex Coil Suite) that employs an exchangeable soft cover, which can be covered by sterile drapes and disposed of after a procedure.

Interventional Protocol and Workflow

The integration of mobile touchscreen tablet devices and wireless communication enabled the radiologist to have control of the MRI scanner at the procedural table (see Fig. 2 and 10c). This obviated the need for scan interruptions or verbal and gestural commands to the MR technician. The gradient noise and resulting communication problems of MRI have recently been addressed with novel silent technology [30, 31] that can be used with standard imaging hardware and could in future eliminate the need for communication systems. However, their suitability for iMRI and achievability of coverage of a large FOV and sufficient frame rates must be further investigated.

The use of a research platform enabled us to design a specific protocol and interface tailored to MRI-guided endovascular interventions. Our tailored rtMRI interface, in combination with the mobile touchscreen device, led to a significant decrease in both complexity and the need for technician-driven scan adjustments. Furthermore, the ability to select the rtFLOW visualization on the fly (similar to Doppler ultrasound) was considered to be useful for pre- and post-interventional assessment and did add only maximum 45 seconds (mean time 32 seconds) to each procedure. These implementations improved the interventional workflow and also reduced the required mean patient table time to 9 minutes and 2 seconds, which is comparable to the X-Ray guided interventions (8 minutes and 42 seconds) that were performed according to the protocol from the local hospital. The length of time taken to perform the MRI-guided procedures was reduced (minimum procedure time: 6 minutes and 33 seconds) as our experience with the setup increased. Further experience and training with our developed framework of technologies could potentially lead to shorter procedure times in future [22, 32].

MRI-guided procedures were also successful with the commercially available rtMRI interface (i/Drive Pro Plus, GE Healthcare, Waukesha, WI, USA). However, workflow interruptions, caused by e.g. stopping the scanner, offline adjustments to pulse sequence parameters and re-starting the scan acquisition, resulted in delays and the mean procedure time was more than double (19 minutes and 58 seconds) than either the X-Ray-guided or MRI-guided procedures with the research protocol.

In this study, all scan plane adjustments were performed manually i.e. to follow an interventional device that was moved out of the current scan plane. Recently, a concept for robust wireless tracking of catheters equipped with resonant markers has been proposed [21]. Integrating this concept into our proposed framework could additionally improve and simplify the interventional workflow, which needs to be assessed in further studies.

This described approach for cardiovascular interventions may be particularly applicable for paediatric and fetal patients or patients with contrast contraindications, as all steps can be performed exclusively under MRI-guidance without the need for contrast agents. Iodinated contrast media are commonly used in X-Ray fluoroscopy-guided procedures and represent one of the main causes of contrast-induced nephropathy and hospital-acquired renal failure [1]. While the risk of radiation injury remains controversial, even low-level exposure is thought to contribute to the long-term risk of malignancy [33]. Paediatric and fetal patients

are considered even more sensitive to radiation and may live longer to experience radiation toxicity [17, 33, 34].

Conclusion

In conclusion, the results of our experiments illustrate the feasibility of our framework developed for guiding endovascular interventions such as common iliac angioplasty, solely with MRI. Dedicated equipment designed for interventions and streamlined workflow can improve the procedural efficacy. Our interactive protocol allowed switching between pulse sequences without interruption of imaging. This provided real-time device manipulation and instant evaluation of technical procedural success, along with adjustments to the treatment protocol on the fly. Accordingly, with our protocol we can also evaluate the implications and response of the treatment to the downstream vasculature. In particular the rtFLOW visualization was found to be helpful for pre- and post-interventional assessment. Although the initial results are encouraging, this feasibility study was conducted in idealized phantom conditions and needs to be repeated in vivo. Future work is planned to investigate this framework in an animal study and in the clinical setting.

Acknowledgments

We thank Leonard Fass and John Ferrut as well as Tom Breslin and Gabor Mizsei for their friendly and helpful support. We are in particular grateful for the help and input from Patricia Seifert, Bernhard Uihlein and Paul Borm. The authors are thankful for financial assistance provided by the FUSIMO (“Patient specific modelling and simulation of focused ultrasound in moving organs”) project funded under the European Community's Seventh Framework Programme (FP7/2007-2013) for Research and Technological Development under Grant Agreement no 270186. The Marie Curie Initial Training Network supported this work and the Integrated Interventional Imaging Operating System (IIIOS) project has received funding from the European Community's Seventh Framework Programme (FP7/2007-2013) under Grant Agreement no 238802.

Conflicts of Interest and Source of Funding: The Integrated Interventional Imaging Operating System (IIIOS) project has received funding from the European Community's Seventh Framework Programme (FP7/2007-2013) under Grant Agreement no 238802. Martin A. Rube, Fabiola Fernandez-Gutierrez, Mahsa Fatahi, Benjamin F. Cox and Andrew B. Holbrook have received funding from the European Union (IIIOS project). Andrew B. Holbrook has also received funding from the following grants NIH R01-CA121163 and P01-CA159992. Helen McLeod has received funding from the European Union (FUSIMO project, Grant Agreement no 270186). Richard D. White has no conflicts of interest. Graeme J. Houston is director, shareholder, patent holder and receives royalty at Tayside Flow Technologies Ltd. Andreas Melzer is consultant and shareholder at INNOMEDIC GmbH, Herxheim, Germany.

REFERENCES

1. Bartorelli AL, Marenzi G. Contrast-induced nephropathy. J Interv Cardiol. 2008; 21:74–85. [PubMed: 18086132]
2. Martin CJ. A review of radiology staff doses and dose monitoring requirements. Radiat Prot Dosim. 2009; 136:140–57.
3. Gedroyc WM. Interventional magnetic resonance imaging. BJU Int. 2000; 86:174–80. [PubMed: 10961287]
4. Schaefers G, Melzer A. Testing methods for MR safety and compatibility of medical devices. Minim Invasive Ther Allied Technol. 2006; 15:71–5. [PubMed: 16754189]
5. Weiss CR, Nour SG, Lewin JS. MR-guided biopsy: a review of current techniques and applications. J Magn Reson Imaging. 2008; 27:311–25. [PubMed: 18219685]
6. Yutzy SR, Duerk JL. Pulse sequences and system interfaces for interventional and real-time MRI. J Magn Reson Imaging. 2008; 27:267–75. [PubMed: 18219681]

7. Smink J, Häkkinen M, Holthuizen R, Krueger S, Ries M, Berber Y, Moonen C, Köhler M, Vahala E. eXTernal Control (XTC): a flexible, real-time, low-latency, bi-directional scanner interface. Proc Intl Soc Mag Reson Med. 2011; 20:1755.
8. Lorenz, CH.; Kirchberg, KJ.; Zuehlsdorff, S.; Speier, P.; Caylus, M.; Borys, W.; Moeller, T.; Guttman, MA. Proc Intl Soc Mag Reson Med. Vol. 13. Miami, FL, USA: 2005. Interactive Frontend (IFE): A platform for graphical MR scanner control and scan automation.; p. 2170
9. Santos, JM.; Wright, G a; Pauly, JM. Conf Proc IEEE Eng Med Biol Soc. San Francisco, CA, USA: 2004. Flexible real-time magnetic resonance imaging framework.; p. 1048-51.
10. Rube, MA.; Seifert, P.; Bernhard, U.; Kakchingtabam, D.; Andre, P.; Melzer, A. Proc Intl Soc Mag Reson Med. Vol. 20. Melbourne: 2012. Novel MR-safe guidewire with passive Iron-Platinum alloy nanoparticles for MR-guided interventions.; p. 4239
11. Guttman MA, Ozturk C, Raval AN, Raman VK, Dick AJ, Desilva R, Karmarkar P, Lederman RJ, Mcveigh ER. Interventional Cardiovascular Procedures Guided by Real-time MR Imaging : An Interactive Interface Using Multiple Slices , Adaptive Projection Modes and Live 3D Renderings. J Magn Reson Imaging. 2007; 1435:1429–1435. [PubMed: 17968897]
12. Melzer A, Michitsch S, Konak S, Schaefers G, Bertsch T. Nitinol in magnetic resonance imaging. Minim Invasive Ther Allied Technol. 2004; 13:261–71. [PubMed: 16754135]
13. Bock M, Wacker FK. MR-guided intravascular interventions: techniques and applications. J Magn Reson Imaging. 2008; 27:326–38. [PubMed: 18219686]
14. Bakker CJ, Hoogeveen RM, Weber J, van Vaals JJ, Viergever M a, Mali WP. Visualization of dedicated catheters using fast scanning techniques with potential for MR-guided vascular interventions. Magn Reson Med. 1996; 36:816–20. [PubMed: 8946346]
15. Burl M, Coutts G a, Young IR. Tuned fiducial markers to identify body locations with minimal perturbation of tissue magnetization. Magn Reson Med. 1996; 36:491–3. [PubMed: 8875424]
16. Bock M, Umathum R, Zuehlsdorff S, Volz S, Fink C, Hallscheidt P, Zimmermann H, Nitz W, Semmler W. Interventional magnetic resonance imaging: an alternative to image guidance with ionising radiation. Radiat Prot Dosim. 2005; 117:74–8.
17. Ratnayaka K, Faranesh AZ, Guttman MA, Kocaturk O, Saikus CE, Lederman RJ. Interventional cardiovascular magnetic resonance: still tantalizing. J Cardiovasc Magn Reson. 2008; 10:62–85. [PubMed: 19114017]
18. Schmidt EJ, Mallozzi RP, Thiagalingam A, et al. Electroanatomic mapping and radiofrequency ablation of porcine left atria and atrioventricular nodes using magnetic resonance catheter tracking. Circ Arrhythm Electrophysiol. 2009; 2:695–704. [PubMed: 19841033]
19. Radau, PE.; Pintilie, S.; Flor, R.; Biswas, L.; Oduneye, SO.; Ramanan, V.; Anderson, KA.; Wright, GA. VURTIGO : Visualization platform for teal-time , MRI-guided cardiac electroanatomic mapping. Camara, O.; Konukoglu, E.; Pop, M.; Rhode, K.; Sermesant, M.; Young, A., editors. STACOM. Springer-Verlag; Berlin Heidelberg, Toronto, Canada: 2011. p. 244-53.
20. Wolska-Krawczyk M, Rube MA, Immel E, Melzer A, Buecker A. Heating and safety of a new MR-compatible guidewire prototype versus a standard nitinol guidewire. Radiol Phys Technol. 2014; 7:95–101. [PubMed: 24203851]
21. Rube MA, Holbrook AB, Cox BF, Melzer A. Wireless MR tracking of interventional devices using phase-field dithering and projection reconstruction. Magn Reson Imaging. [E-Pub ahead of print]. doi: 101016/j.mri.2014.03.007.
22. Fernández-Gutiérrez F, Barnett I, Taylor B, Houston G, Melzer A. Framework for detailed workflow analysis and modelling for simulation of multi-modal image-guided interventions. J Enterp Inf Manag. 2013; 26:75–90.
23. Du YP, Parker DL, Davis WL, Cao G. Reduction of partial-volume artifacts with zero-filled interpolation in three-dimensional MR angiography. J Magn Reson Imaging. 1994; 4:733–41. [PubMed: 7981519]
24. Immel E, Melzer A. Improvement of the MR imaging behavior of vascular implants. Minim Invasive Ther Allied Technol. 2006; 15:85–92. [PubMed: 16754191]
25. Kaiser M, Detert M, Rube MA, Eldirdiri A, Elle OJ, Melzer A, Schmidt B, Rose G. Resonant marker design and fabrication techniques for device visualization during interventional magnetic resonance imaging. Biomed Tech. 2013 [in review].

26. Rube, MA.; Immel, E.; Toomey, R.; Wolska-Krawczyk; Melzer, A. Semi-active resonant markers for interventional device localization in real-time MR Imaging.. In: Szold, A.; Shoham, M., editors. Proc 23rd Conf Soc Med Innov Technol; Tel Aviv, Israel. 2011. p. SSG17-07.
27. Konings MK, Bartels LW, Smits HF, Bakker CJ. Heating around intravascular guidewires by resonating RF waves. J Magn Reson Imaging. 2000; 12:79–85. [PubMed: 10931567]
28. Nitz WR, Oppelt A, Renz W, Manke C, Lenhart M, Link J. On the heating of linear conductive structures as guide wires and catheters in interventional MRI. J Magn Reson Imaging. 2001; 13:105–14. [PubMed: 11169811]
29. Rothgang E, Gilson WD, Wacker F, Hornegger J, Lorenz CH, Weiss CR. Rapid freehand MR-guided percutaneous needle interventions: An image-based approach to improve workflow and feasibility. J Magn Reson Imaging. 2013; 37:1202–12. [PubMed: 23334924]
30. Weiger M, Brunner DO, Dietrich BE, Müller CF, Pruessmann KP. ZTE imaging in humans. Magn Reson Med. 2013; 70:328–32. [PubMed: 23776142]
31. Grodzki, DM.; Heisman, B. Proc Intl Soc Mag Reson Med. Vol. 21. Salt Lake City, UT, USA: 2013. Quiet T1-weighted head scanning using PETRA.; p. 456
32. Hoffmann R, Thomas C, Rempp H, Schmidt D, Pereira PL, Claussen CD, Clasen S. Performing MR-guided biopsies in clinical routine: factors that influence accuracy and procedure time. Eur Radiol. 2012; 22:663–71. [PubMed: 21960160]
33. Kleinerman, R a. Cancer risks following diagnostic and therapeutic radiation exposure in children. Pediatr Radiol 36 Suppl. 2006; 2:121–5.
34. Mathews JD, Forsythe a. V. Brady Z, et al. Cancer risk in 680 000 people exposed to computed tomography scans in childhood or adolescence: data linkage study of 11 million Australians. BMJ. 2013 doi: 101136/bmj.f2360.

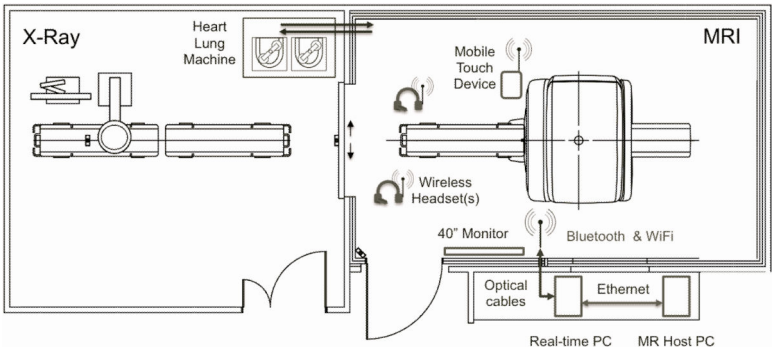

Fig. 1.

Floor plan of the multi-modality setup including modifications – Modifications included rtMRI image display, in-room MRI remote control, communication and the heart-lung machine (HL-30, Maquet, Rastatt, Germany) for vascular perfusion. The left room contains a digital subtraction angiographic unit (OEC 9900 Elite, GE Healthcare Systems, Waukesha, WI, USA) and the right room is an RF shielded enclosure with a clinical 1.5 T MRI scanner (Signa HDxt, GE Healthcare, Waukesha, WI, USA). The rooms are interconnected with sliding doors, that shield RF and radiation and allow a patient transfer on a mobile table with radiolucent sliding table top (MR 1050 surgical suite, GE Healthcare and Maquet, Rastatt, Germany)

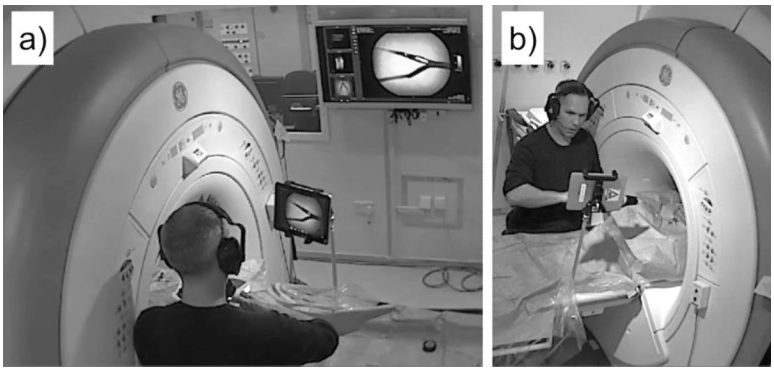

Fig. 2.

Photographs taken during a MRI-guided iliac angioplasty procedure demonstrating the in-room iMRI display and control setup - The pictures were taken from two wireless IP cameras (M1031W, Axis, Lund, Sweden) that were installed in the scanner room. The picture (a) was acquired from the back and picture (b) from the front. The mobile tablet was mounted on an IV pole. The screen of the tablet shows the same rtMRI scene as the 40″ in-room monitor. Note that the physician was able to zoom (a) into the region of interest on the touchscreen

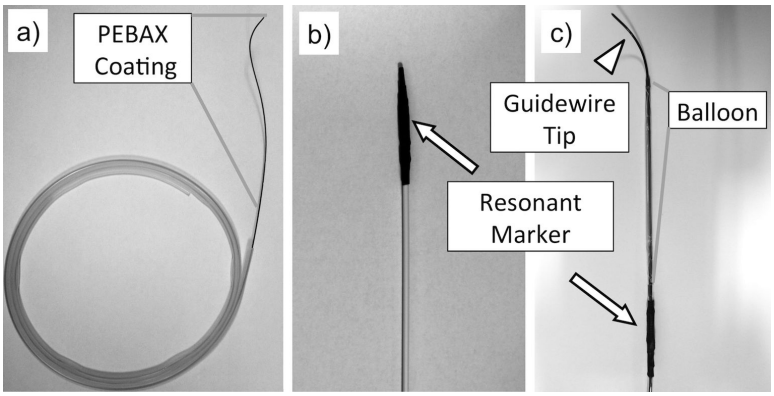

Fig. 3.

Photographs showing the interventional devices prepared for iMRI visualization – a) The MR safe guidewire, b) the straight catheter with a resonant tip marker (arrow) and c) the balloon catheter with the inserted guidewire (arrowhead) and a resonant marker (arrow) positioned behind the non-inflated balloon

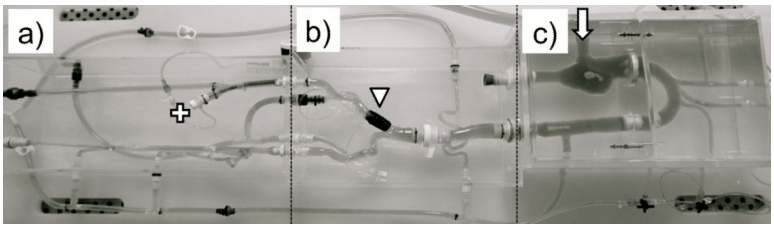

Fig. 4.

Photograph of the arterial phantom setup - The vessels were perfused with food colouring for optimized visualization and demonstration: The model consisted of three connected modules: a leg model (a) - full left leg and a simplified right leg, an abdominal model (b) and a rigid thoracic phantom (c) (L-F-S-Left-003, A-S-N-001, T-R-N-020, Elastrat, Sarl, Switzerland). The master arterial pump of the heart lung machine (HL-30, Maquet, Rastatt, Germany) was connected to cardiac chamber of the thoracic phantom and the arrow indicates the inflow. The '+' indicates the 12-F introducer sheath for vascular access and the arrowhead indicates the neonatal pressure cuff (SoftCheck Neonatals, Statcorp Medical, Jacksonville, FL, USA) that was attached to the right common iliac artery to mimic a stenosis

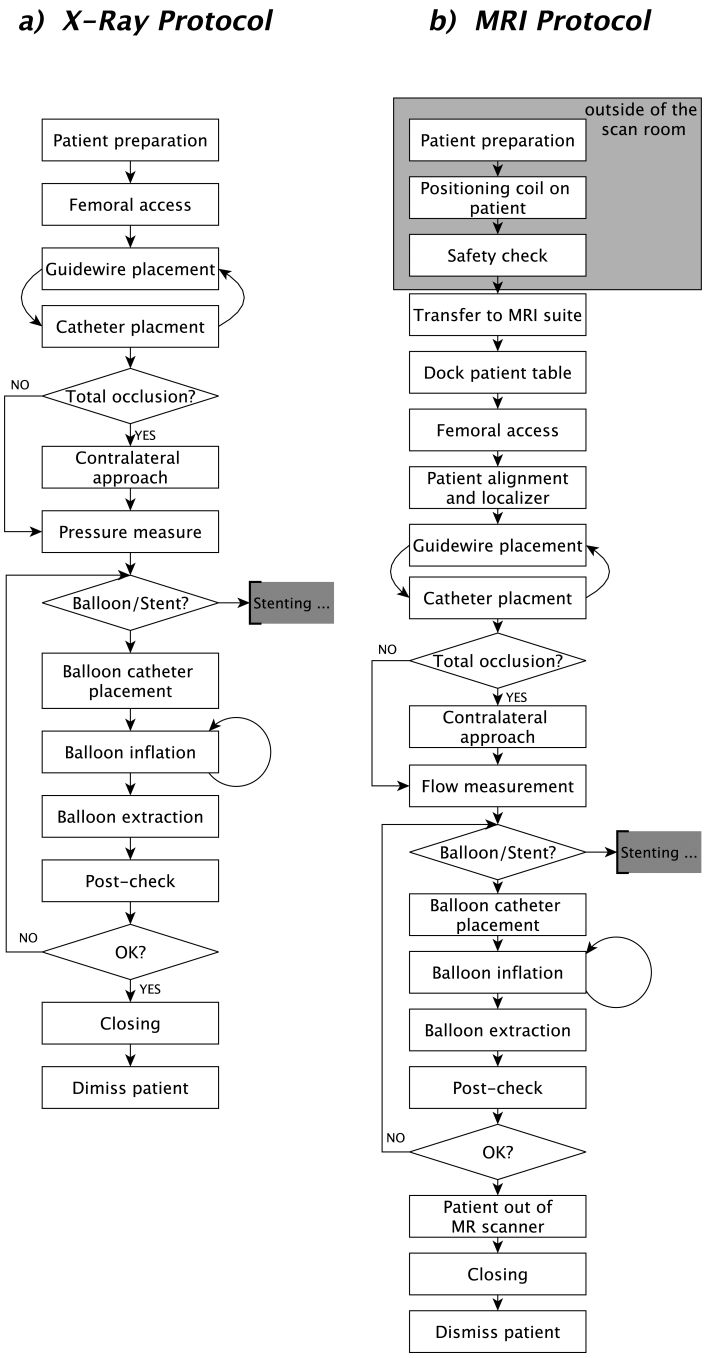

Fig. 5.

Flow diagram of the common iliac angioplasty protocol - a) Standard protocol applied in the interventional radiology department of the local for X-Ray-guided balloon angioplasties and b) the adapted protocol for MRI guided-interventions

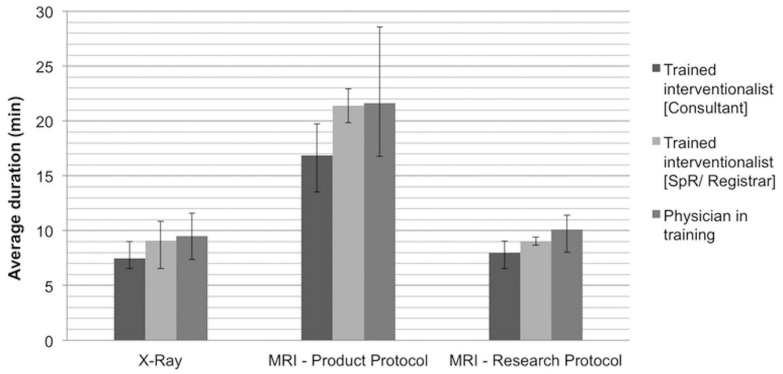

Fig. 6.

Average procedure times and range (illustrated as bars) for the performed interventions categorized by setup/protocol - The vertical axis displays the average time in minutes, from the first localizer until the patient (phantom) was taken off the MRI patient table. The three columns separate the operating physicians. The first set of columns is the mean time for the X-Ray-guided procedures that were performed as reference. Each physician performed three independent X-Ray-guided iliac angioplasties. The second and third set of columns shows the MRI-guided interventions. The second set of columns shows the average procedure time for the product protocol (n = 5 per physician) and the last set of columns shows the MRI-guided iliac angioplasties performed with the advanced research protocol (n = 5 per physician)

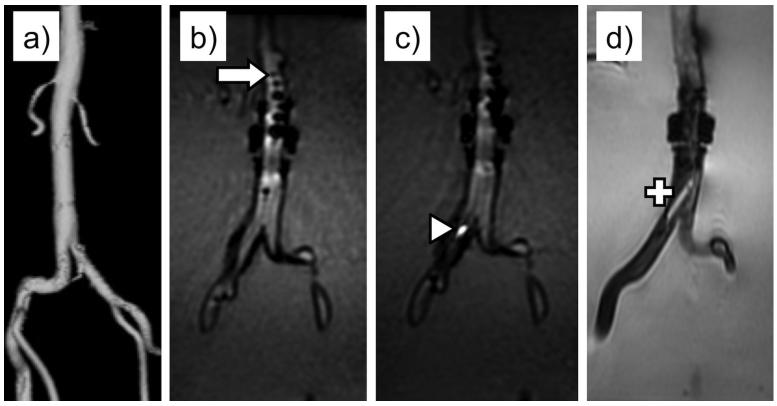

Fig. 7.

MR images of the devices positioned in the common iliac artery obtained with the product rtMRI interface (i/Drive Pro Plus, GE Healthcare, Waukesha, WI, USA) - (a) Pre-interventional MIP of the 2D ToF MRA showing the abdominal aorta and the iliac arteries without any device present, (b) shows the tip section of the MRI-safe guidewire (the arrow indicates the tip) that was positioned in the aorta, (c) the white spot (arrowhead) at the level beginning of the iliac arteries shows is the resonant marker on the straight catheter, (d) inflated balloon (+) catheter (with 1:100 Gd-doped saline solution) that was moved just above the common iliac artery and required re-positioning. Please note, the signal void outside the lumen of the aorta is due to the connector that allows exchanging different renal vessel models and is not an artefact

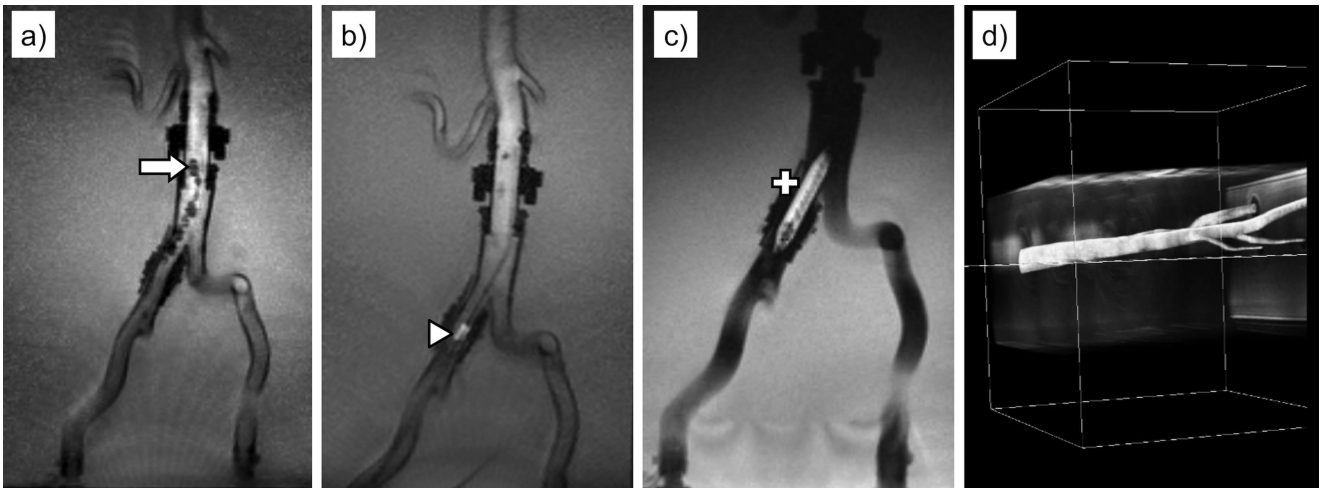

Fig. 8.

MR images of device placements in the common iliac artery obtained with the developed real-time interface and customized interventional protocol - image (a) shows the tip section of the MRI-safe guidewire (the arrow indicates the tip) with the susceptibility artefacts of each distinct passive marker. Image (b) displays the straight catheter with the resonant tip marker (arrowhead) at the level of the iliac arteries. On image (c) the inflated balloon catheter (+) with 1:100 Gd-doped saline solution, positioned in the right common iliac artery, can be depicted. Image (d) demonstrates a post-interventional MIP of a 2D ToF MRA with treated stenosis in the right common iliac artery

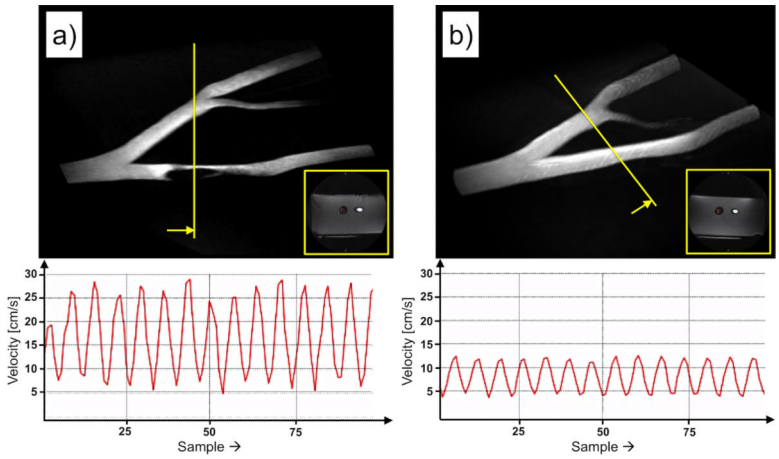

Fig. 9.

Flow/velocity examination performed in real-time and at various segments of the common iliac artery - The flow study at the level of the stenosis is shown exemplarily before (a) and after the stenosis treatment (b). The arrows in the MIP dataset (2D ToF) indicate the orientation of the flow-encoded axial images (rtFLOW) that are shown in the frame in the lower right corner of the MIP dataset. The flow patterns below the two MIP datasets are also obtained with real-time phase contrast MRI and demonstrate the velocity profile averaged over a region of interest (ROI), which was positioned within the vessel segment of interest (ROI not shown for simplicity)

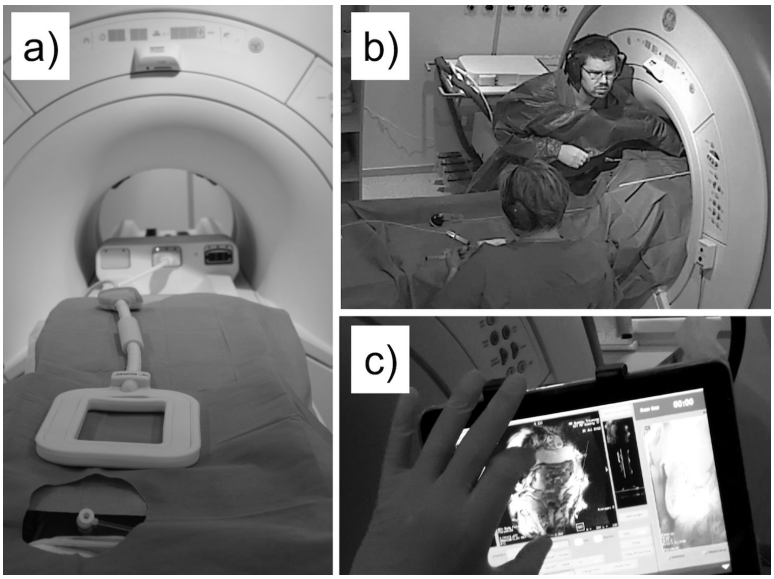

Fig. 10.

Intra-procedural photographs demonstrating the setup and modifications - Image (a) shows the vascular access and the single loop element of the dedicated interventional coil positioned on top of the right common iliac artery. Image (b) shows the physician and nurse during catheter placement during an MRI-guided common iliac angioplasty. Image (c) shows how the physician can zoom into the area of interest during rtMRI using the tablet device with latex glove

TABLE 1

Summary of the MR imaging parameters for the product protocol

	Diagnostic MRI		Interactive rtMRI	
	FSPGR	**2DToF**	**FGRE**	**FSPGR**
TR/TE (ms)	2.0/4.5	2.6/7.5	1.7/4.8	1.8/5.9
Field of view (FOV) (CM)	40	35	40	40
Matrix	256 × 256	320 × 192	256 × 128	256 × 128
Flip Angle (°)	70	70	30	70
Slice thickness (mm)	7	7	7	7

TABLE 2

Summary of the MR imaging parameters for the research protocol

	Diagnostic MRI		**Interactive rtMRI**			
	FSPGR	**Spiral bSSFP (MRA)**	**rtFLOW (5 interleaves**	**bSSFP**	**Spiral bSSFP (6 interleaves)**	**FGRE**
TR/TE (ms)	2.0/4.5	3.5/21.5	4.9/23.5	4.8/6.9	3.5/20.0	3.0/7.4
Field of view (FOV) (CM)	40	24	24	40	40	24
Matrix	256 × 256	(Resolution 1.76 mm)	(Resolution 1.76 mm)	256 × 256	(Resolution 1.76 mm)	256 × 256
Flip Angle (°)	70	70	30	70	70	≤30/60
Slice thickness (mm)	3	7	5	5	7	5